



Characterization of the hydrogen emission in divertor II of ASDEX-Upgrade

U. Wenzel^{a,*}, K. Behringer^b, K. Büchl^b, A. Herrmann^b, K. Schmidtman^b

^a Max-Planck-Institut für Plasmaphysik (IPP), EURATOM Association, Division Plasma Diagnostics, Mohrenstr. 41, D-10117 Berlin, Germany

^b Max-Planck-Institut für Plasmaphysik (IPP), EURATOM Association, Boltzmannstr. 2, D-85748 Garching, Germany

Abstract

Detailed experiments have been carried out in ASDEX-Upgrade to characterize detached plasma conditions in divertor II. This paper presents measurements of the hydrogen emission in the visible and VUV spectral range that distinguishes between the ionization front and the recombining divertor plasma. Plasma parameters in the recombination dominated region were obtained from the Balmer continuum and line emission. By means of the ADAS programme package the rate of volume recombination is evaluated including the effect of opacity. The optical thickness was experimentally determined from the line ratio of L_{β} and H_{α} . In the recombining plasma we have observed an inverse response of H_{α} light during the spatial broadening of ELMs. Inverse ELMs show signatures of convective transport. © 1999 Elsevier Science B.V. All rights reserved.

Keywords: ASDEX-Upgrade; Divertor spectroscopy; ELM; Opacity; Recombination

1. Introduction

Volume recombination can be a substantial sink of plasma ions in the divertor. The plasma conditions necessary for a significant recombination rate were first discovered on Alcator C-Mod using spectroscopical methods ($T_e = 1$ eV and $n_e = 10^{21} \text{ m}^{-3}$) [1]. Similar plasma parameters were found in divertor I of ASDEX-Upgrade by four different methods. For the measurement of the electron density the half width of Balmer lines and the absolute intensity of the Balmer continuum was used. The electron temperature was determined from the Lyman continuum and by the method of the Balmer sprung. For the inboard divertor it was shown that the volume recombination rate exceeds the ion collection rate at the plate. Here the recombination sets in first due to an in-out asymmetry of the electron temperature.

In the new divertor of ASDEX-Upgrade (divertor II) volume recombination is already significant at lower

line-averaged density than in divertor I due to geometrical effects [2]. The investigation of the Balmer and Lyman series was continued to study the following items connected with the recombination dominated zone:

- Distinction of the ionizing and recombining region of the divertor.
- Opacity of the Lyman series in the recombining plasma.
- Measurement of the plasma parameters with high spatial resolution.
- Occurrence of an inverse response to ELMs in the recombining plasma.

2. Experimental

The divertor spectroscopy in ASDEX-Upgrade comprises a multi-chord spectrometer for the visible range (divertor spectrometer) and a spatially scanning, combined VUV- and visible range instrument (boundary layer spectrometer [3]). For the investigation of ELMs a special diode array operating with H_{α} filters was used. The lines of sight of the latter are shown in Fig. 1 together with four channels of the divertor spectrometer

* Corresponding author. Tel.: +49 30 20 366; fax: +49 30 20 366 111; e-mail: wenzel@ipp.mpg.de

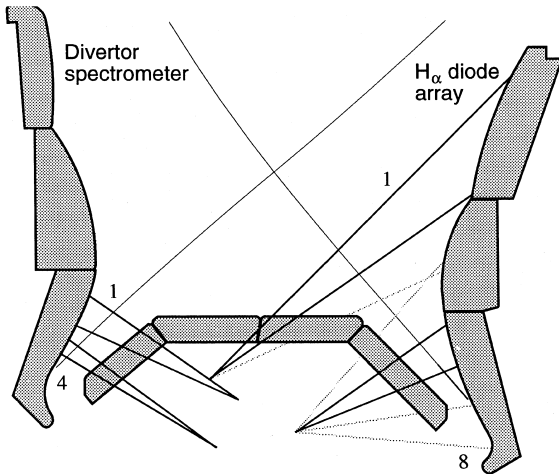


Fig. 1. Four lines of sights of the divertor spectrometer (inboard) used for the measurement of the plasma parameters and the diode array in the outboard divertor used for ELM studies in H α light.

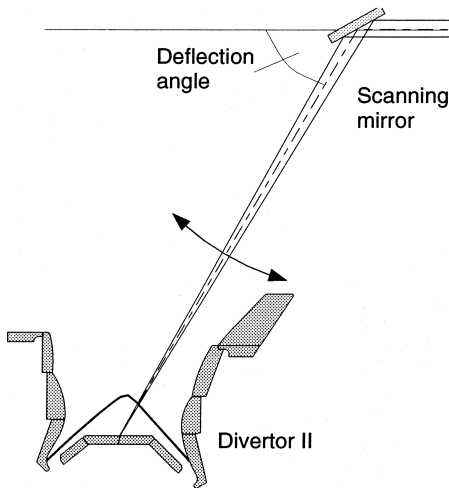


Fig. 2. Boundary layer spectrometer for the VUV and visible ranges. The inboard divertor is scanned when the deflection at the scanning mirror amounts to -55° . At -65° the line of sight strikes the outboard divertor baffle.

used for the study of the Balmer series in the inboard divertor. Fig. 2 shows the lines of sight of the boundary layer spectrometer when it scans the divertor. Intensity profiles are plotted over the deflection angle of the mirror.

3. Ionization front and recombining region

During the study of the Lyman series it was found that the emission peak of L_α differs from the maxima of

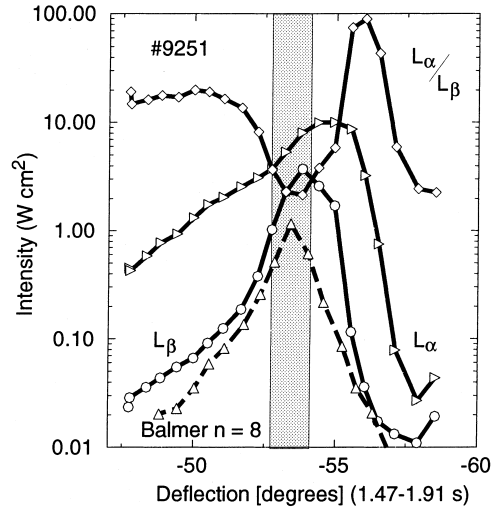


Fig. 3. Spatial profile of the L_α , L_β and Balmer $n=8$ emission in the inboard divertor measured with the boundary layer spectrometer. By means of the ratio L_α/L_β the ionization front with a value of 80 can be distinguished from the recombining region where it is 2. The recombining region is emphasized by the gray box. Its width amounts to 1.3° corresponding to 3.6 cm.

all other hydrogen lines including the lines of the Balmer series. Fig. 3 shows the emission of three hydrogen lines from the inner divertor (L_α , L_β and the Balmer line $n=8$) over the deflection angle of the scanning mirror. Also shown is the ratio of the lines from the Lyman series. This ratio is about 2 at -53.8° and increases up to values of 80 at -55.9° . The emission of the Balmer line which is only observed when volume recombination prevails is similar to the L_β profile. For plasma parameters of $T_e = 1$ eV and $n_e = 10^{21} \text{ m}^{-3}$ the collisional limit of the energy levels is between the quantum numbers 2 and 3. Levels with $n \geq 3$ are mainly coupled to the continuum which explains the observed similarity of the Balmer $n=8$ and L_β spatial profile.

Other considerations apply for the ratio L_α and L_β . L_α is not only observed in the recombination region but also in hotter regions where the level with $n=2$ is populated by excitation from the ground state. Theoretical values for the line ratio are shown in Fig. 4 calculated with the collisional-radiative model of Johnson and Hinnov [4]. The ratio is plotted for different coupling cases: with coupling to the ground state alone (excitation from ground state), with coupling to the continuum alone (recombination) and with both. The calculations show above 3 eV line ratios between 30 and 60 independent of recombination. Below 1 eV the line ratio varies between 3 and 1.5. Here it does not depend on the excitation from ground state. In the transition range between 1 and 3 eV the line ratio is a strong function of the electron temperature. Note, that the width of the transition region is determined by the neutral density

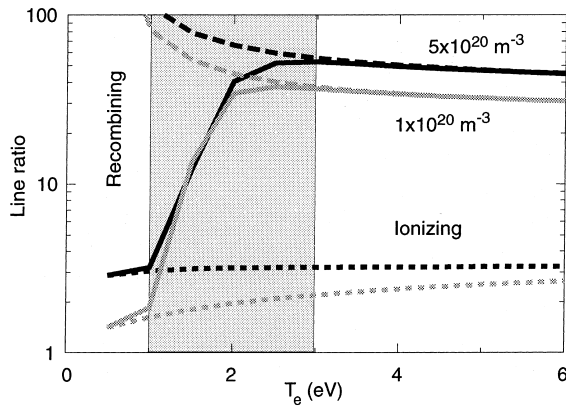


Fig. 4. Theoretical line ratio L_α to L_β for two values of the plasma density. Also shown are the limits recombining (dotted line) and ionizing plasma (dashed line). The neutral density was assumed to be 10% of the ion density. Outside a transition region (between 3 and 1 eV) the line ratio depends little on the plasma parameters. In the transition region (gray box) both recombination and excitation influence the line ratio. Here it is a sensitive function of the temperature. For this analysis optically thin conditions were assumed.

which was assumed to be 10% of the plasma density. This assumption will be justified later by the estimation of the neutral density from the self-absorption of the Lyman series.

In the experimental profile we are now able to distinguish between the recombining region (with $T_e < 1$ eV) and the ionizing region located upstream (with $T_e > 3$ eV). In the transition region between -55.5° and -53.8° the temperature drops below 1 eV.

4. Optical thickness

Owing to volume recombination in the divertor the neutral density becomes high enough to trap the hydrogen resonance lines. This was already demonstrated in divertor I of ASDEX-Upgrade by the detection of a non-proportional increase of H_α and L_β during a density ramp [5]. Results for the new divertor configuration are presented in Fig. 5. Density and power were simultaneously ramped up to hold the L mode. Hydrogen emission from the inboard divertor is sampled by the scanning spectrometer. Above a line-averaged density of $5.6 \times 10^{19} \text{ m}^{-3}$ L_β does not track H_α . Escape factors for L_β range between 0.66 and 0.76.

Model calculations show that such factors are expected for line integrals of the neutral density in the interval from $1.8 \times 10^{18} \text{ m}^{-2}$ to $1 \times 10^{18} \text{ m}^{-2}$ [6]. At these densities L_α is strongly trapped. Under opaque conditions the net recombination is influenced for electron temperatures between 1 and 1.5 eV. In this tem-

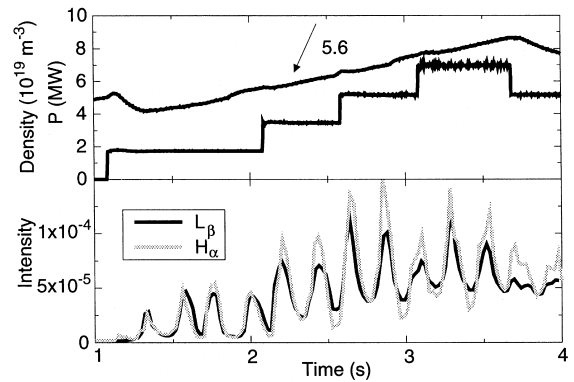


Fig. 5. Emission of H_α and L_β vs. time during density ramp-up. The inboard divertor is scanned. The emission peaks when the line of sight strikes the recombination region. Above $5.6 \times 10^{19} \text{ m}^{-3}$ L_β does not track H_α , i.e. the plasma becomes opaque.

perature range the recombination rate is reduced by approximately a factor of 3 in comparison to the optically thin case. Furthermore, by an increase of the ionization rate by the same amount the onset of net recombination is shifted to temperatures below 1 eV. When a significant net recombination is required to interpret the Langmuir probe measurements, the electron temperature must not exceed 1 eV. The effect of opacity has been neglected in the analysis of the line ratio L_α/L_β in the preceding section because the line-averaged density was below the detection threshold of $5.6 \times 10^{19} \text{ m}^{-3}$.

5. The recombining divertor plasma

The measurement of the continuous and line emission of hydrogen in the visible spectral range with the divertor spectrometer enables one to determine the plasma parameters. Fig. 6 shows the results for the inboard divertor obtained with the method of the Boltzmann plot (T_e) and from the absolute intensity of the Balmer continuum (n_e). An extension of the emission zone of 3.6 cm, determined from the top view by the boundary layer spectrometer, was used for the evaluation. In the analyzed discharge neutral beam power and density were ramped-up very similar to the discharge shown in Fig. 5. We consider the plateau with 7 MW heating power by neutral beams. At a line-averaged density of $8.5 \times 10^{19} \text{ m}^{-3}$ (at 3.0 s) the inner divertor is detached as indicated by the flat temperature profile with 0.3 eV while the outer is still attached. When the line-averaged density has reached $9.2 \times 10^{19} \text{ m}^{-3}$ (at 3.5 s) MARFE formation is observed near the X-point. The occurrence of the MARFE triggers the detachment of the outer divertor and additional pressure loss in the inner divertor (see the corresponding density profile in

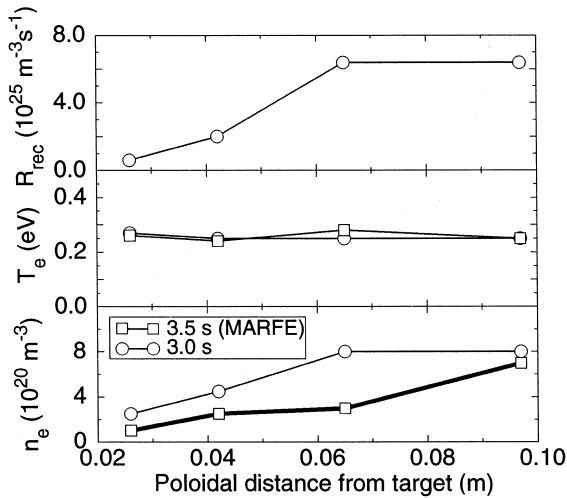


Fig. 6. Plasma parameters and volume recombination rates in the inner divertor. The target is located at $x=0$. We observe a constant electron temperature at 0.3 eV. Due to the high volume recombination rate the density drops toward the target plate. To explain the density profile, we have to assume a slowing down of the plasma flow. Note that the ionization front was outside the spectrometer channels.

Fig. 6). Plasma parameters in the MARFE are very similar to the recombining divertor plasma as found by spectroscopic measurements from the top view. Along the separatrix the plasma density drops toward the target at $x=0$. The reason is the strong volume recombination in front of the plate. We have calculated recombination rate coefficients using the ADAS programme. There is only little variation of the recombination rate coefficient for $T_e = 0.3$ eV considering the opacity but it is proportional to the electron density because of three-body recombination. Fig. 6 shows the volume recombination rate as function of the distance from the target calculated with a constant rate coefficient of $10^{-16} \text{ m}^3 \text{ s}^{-1}$ and the measured density. Volume recombination is maximum 0.1 m from the target due to the high plasma density. However, a decrease of the plasma density is only observed immediately in front of the target where the rates are a factor of 10 lower. To match the plasma density and the volume recombination rates a slowing down of the plasma flow must be assumed.

6. Inverse ELMs and convective transport

Bursts of energy due to ELMs may temporarily heat the SOL. The energy is rapidly conducted parallel to the field lines into the divertor. ELMs are detected by a short increase of optical signals. When heat conduction prevails they are in phase because transport times are

small compared to the duration of an ELM. In the recombining divertor, however, quite different observations were made when investigating the H_α signal.

Consider a H-mode discharge in which the density was ramped-up. Fig. 7 shows the H_α signals from the outer divertor for a density of $5.5 \times 10^{19} \text{ m}^{-3}$ (at 2.2 s) and $7.0 \times 10^{19} \text{ m}^{-3}$ (at 2.6 s), respectively. The lines of sight are shown in Fig. 1. At low density the ELM signal behaves as described above. All lines of sight detect simultaneously an increase of the H_α emission. At high density, however, ELMs cause a reduction of the emission deep in the divertor (see channel 6) where a recombining region was formed. Lines of sight crossing the upper ionizing region (channels 1 and 2) still behave as before. Additionally, a phase shift between the H_α signals from both zones is observed.

A burst of particles during an ELM increases the H_α emission. Therefore, a reduction must be a temperature effect. Calculations with the collisional-radiative model of Johnson and Hinnoy show a minimum of the H_α emission between 1 and 2 eV, i.e. at the transition from ionizing to recombining conditions. We conclude that an inverse ELM occurs when a burst of energy spreads through a recombining plasma increasing the electron temperature above 1 eV for a short time.

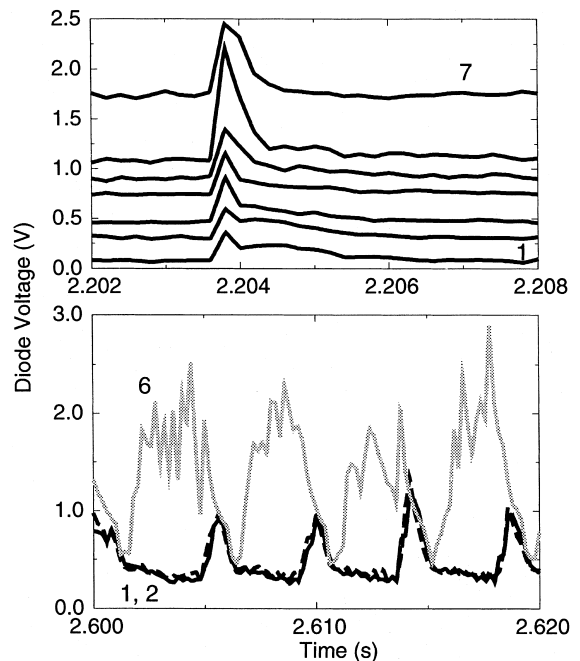


Fig. 7. Spatial broadening of ELMs through an attached plasma (channels 1–7, on top) and a detached plasma (channels 1, 2 and 6, at bottom). In the region with significant volume recombination inverse ELMs occur (see channel 6 at bottom). In the first case the energy is transported by conduction, in the second by convection as indicated by the phase shift.

How is the energy transported in the recombining plasma? Heat conduction is inefficient at low electron temperature. Convection explains the energy transport in a manner consistent with the H_{α} measurements. The phase shift between the maximum from channel 2 and the minimum from channel 6 (0.5 ms) points to slow energy transport in comparison to the upper part of the divertor, where the signals are in phase (see channel 1 and 2). Taking the length between channel 2 and 6 along the field lines (4 m) we get a phase velocity of 8×10^3 m/s which is in the order of the sound velocity at 1 eV. Convection was also identified in the divertor of DIII-D to be the primary mechanism for energy transport by a direct measurement of the radiative losses and the plasma parameters [7].

7. Summary

By a measurement of the emission of the Lyman series divertor regions were distinguished where either purely ionizing (above 3 eV) or recombining conditions (below 1 eV) prevail. A measurement of the temperature in the recombining region of the inner divertor by the method of the Boltzmann plot shows a flat profile along the separatrix with 0.3 eV. The electron density decreases toward the target plate due to strong net recombination in the plasma volume with rates in the order of $10^{25} \text{ m}^{-3} \text{ s}^{-1}$. The resulting high neutral density causes the first lines of the Lyman series to become opaque. For L_{β} , optically thick conditions have been detected at densities above $5.6 \times 10^{19} \text{ m}^{-3}$. From the degree of self absorption the mean neutral density was estimated to $2 \times 10^{19} \text{ m}^{-3}$. In the recombining divertor

plasma, H_{α} shows an inverse response during an ELM. Inverse ELMs occur when the energy bursts increase the temperature to values above 1 eV for a short time. The observed phase shift between different measurement channels points clearly to convective energy transport.

References

- [1] D. Lumma, J. Terry, B. Lipschultz, *Phys. Plasmas* 4 (7) (1997) 2555.
- [2] R. Schneider et al., these Proceedings.
- [3] A.R. Field, J. Fink, R. Dux, G. Fussmann, U. Schumacher, U. Wenzel, *Rev. Sci. Instrum.* 66 (1995) 5433.
- [4] L. Johnson, E. Hinnov, *J. Quant. Spectrosc. Radiat. Transfer* 12 (1973) 333.
- [5] B. Napiontek, U. Wenzel, K. Behringer, D. Coster, J. Gafert, R. Schneider, A. Thoma, M. Weinlich, and ASDEX Upgrade Team, Line and recombination emission in the ASDEX Upgrade divertor at high density, in: M. Schittenhelm, R. Bartiromo, F. Wagner (Eds.), *Europhysics Conference Abstracts (Proceedings of the 24th EPS Conference on Controlled Fusion and Plasma Physics, Berchtesgaden, 1997)*, vol. 21A, Part IV, Petit-Lancy, 1997, EPS, pp. 1413–1416.
- [6] K. Behringer, The influence of opacity on hydrogen line emission and ionisation balance in high density divertor plasmas, IPP Report 10/5, Max-Planck-Institut für Plasmaphysik, Garching, BRD, 1997.
- [7] A. Leonard, S. Allen, N. Brooks, T. Evans, M. Fenstermacher, D. Hill et al., Energy and particle transport in the radiative divertor plasma of DIII-D, in: M. Schittenhelm, R. Bartiromo, F. Wagner (Eds.), *Europhysics Conference Abstracts (Proceedings of the 24th EPS Conference on Controlled Fusion and Plasma Physics, Berchtesgaden, 1997)*, vol. 21A, Part IV, Petit-Lancy, 1997, EPS, pp. 1109–1112.